NMR Investigation of Mithramycin A Binding to d(ATGCAT)$_2$: A Comparative Study with Chromomycin A$_3$[†]

Debra L. Banville,[‡] Max A. Keniry,[§] and Richard H. Shafer*,[‡]

Department of Pharmaceutical Chemistry, School of Pharmacy, University of California, San Francisco, California 94143, and Research School of Chemistry, Australian National University, Canberra, ACT 2601, Australia

Received April 18, 1990; Revised Manuscript Received June 22, 1990

ABSTRACT: The binding of mithramycin A to the d($A_1T_2G_3C_4A_5T_6$) duplex was investigated by ^{1}H NMR and found to be similar to that of its analogue chromomycin A$_3$. In the presence of Mg^{2+}, mithramycin binds strongly to d(ATGCAT)$_2$. On the basis of the two-dimensional NOESY spectrum, the complex formed possesses C_2 symmetry at a stoichiometry of two drugs per duplex (2:1) and is in slow chemical exchange on the NMR time scale. NOESY experiments reveal contacts from the E-pyranose of mithramycin to the terminal and nonterminal adenine H2 proton of DNA and from the drug hydroxyl proton to both G3NH$_2$ protons, C4H1′ proton, and A5H1′ proton. These data place the drug chromophore and E pyranose on the minor groove side of d(ATGCAT)$_2$. NOE contacts from the A-, B-, C-, and D-pyranoses of mithramycin to several deoxyribose protons suggest that the A- and B-rings are oriented along the sugar–phosphate backbone of G_3-C_4, while the C- and D-rings are located along the sugar–phosphate backbone of A_5-T_6. These drug–DNA contacts are very similar to those found for chromomycin binding to d(ATGCAT)$_2$. Unlike chromomycin, the NOESY spectrum of mithramycin at the molar ratio of one drug per duplex reveals several chemical exchange cross-peaks corresponding to the drug-free and drug-bound proton resonances. From the intensity of these cross-peaks and the corresponding diagonal peaks, the off-rate constant was estimated to be 0.4 s^{-1}. These data suggest that the exchange rate of mithramycin binding to d(ATGCAT)$_2$ is faster than that of chromomycin.

Mithramycin and chromomycin belong to a group of chemically related antitumor antibiotics that inhibit both DNA and RNA synthesis in vivo (Kersten et al., 1966; Kennedy et al., 1968; Baguley, 1982). These derivatives of aureolic acid possess structural similarities such as a chromomycinone moiety with five hexapyranoses attached (Figure 1; Thiem & Meyer, 1979, 1981). In vitro studies demonstrated that each drug binds to double-stranded regions of DNA, but only in the presence of divalent cations (e.g., Mg^{2+} or Mn^{2+}; Kersten et al., 1966; Ward et al., 1965; Van Dyke & Dervan, 1983). DNA binding also requires the presence of guanine or a 2-aminopurine substituent (Miller et al., 1987; Prasad & Nayak, 1976; Zimmer & Wahnert, 1986; Kersten et al., 1966; Behr et al., 1969; Ward et al., 1965; Baguley, 1982). On the basis of recent footprinting studies, the size of a recognition site is at least three base pairs for both chromomycin and mithramycin (Van Dyke & Dervan, 1983; Fox & Howarth, 1985; Cons & Fox, 1989).

Our earliest one-dimensional NMR studies on chromomycin binding to calf thymus DNA and poly[d(G-C)] confirmed this drug's preference for G-C base pairs (Berman et al., 1985; Berman & Shafer, 1983). Furthermore, these studies demonstrated for the first time the effect of chromomycin binding on the DNA imino protons and provided evidence that the phenolic proton on the chromomycinone ring played an important role in drug binding. Our latest study, utilizing two-dimensional NMR techniques, on chromomycin binding to synthetic deoxyribonucleotides has confirmed and extended these findings (Banville et al., 1990). We demonstrated a base selectivity for 5′-GC-3′ over 5′-CG-3′ sites within a series of DNA sequences, d(ATCCAT)$_2$, d(ATCGAT)$_2$, d(TATGCATA)$_2$, and d(ATAGCTAT)$_2$. Each of the three-GC-containing DNA duplexes has a single binding site that accommodates two drugs and one Mg^{2+} ion. These three drug-DNA complexes possess C_2 symmetry, which greatly simplifies the NMR spectrum. Weak NOE[1] contacts possibly place the B-hexapyranose near the vicinity of the guanine H8 on the major groove side of DNA. Strong NOE contacts from the DNA duplexes to the chromophore and the E-hexapyranose unambiguously place a major portion of the drug tightly in the minor groove of the -GC- containing sequences. A widening of the minor groove is essential for the DNA duplex to accommodate two drug molecules, and evidence for this is apparent in the NOESY spectrum of the chromomycin–d(ATGCAT)$_2$ complex. Similar changes in the minor groove were noted by Scott et al. (1988) for two closely placed actinomycin D molecules bound to d(ATGCGCAT)$_2$ and more recently by Gao and Patel (1989a,b) in their study with the chromomycin–d(TTGGCCAA)$_2$ complex.

Unlike chromomycin, mithramycin does not contain acetyl or methoxy substitutes on the hexapyranoses. Furthermore, mithramycin has a pK_a of 5, which is substantially lower than that of chromomycin at 7 (Illarionova et al., 1970). Footprinting studies do show slight differences in the sequence selectivity of the two drugs (Van Dyke & Dervan, 1983; Fox & Howarth, 1985), while sedimentation studies show different effects on the unwinding of supercoiled DNA (Waring, 1970). However, no structural data are available to assess these differences. Hence, the purpose of this study is twofold: to establish the structural characteristics of mithramycin binding

[†] Supported by NIH Grant CA27343.

[‡] University of California.

[§] Australia National University.

[1] Abbreviations: MRA, mithramycin; CRA, chromomycin A$_3$; NOE, nuclear Overhauser enhancement; NOESY, two-dimensional nuclear Overhauser exchange spectroscopy; COSY, two-dimensional double quantum filtered correlation spectroscopy; HOHAHA, two-dimensional homonuclear Hartmann–Hahn relay spectroscopy.

0006-2960/90/0429-9294$02.50/0

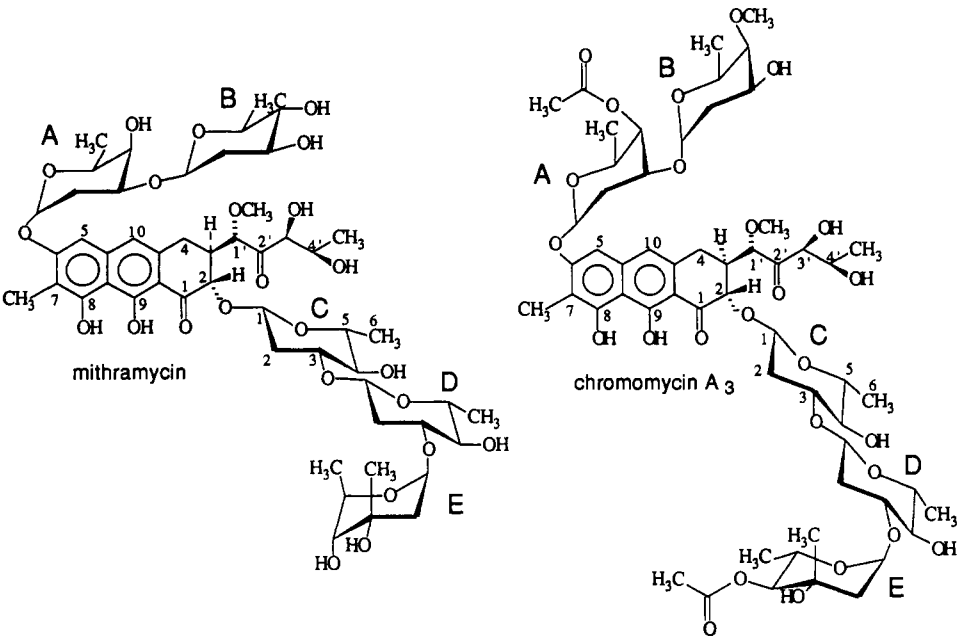

FIGURE 1: Structures of mithramycin A and chromomycin A_3 as determined by Thiem and Meyer (1981, 1979).

to the -GC- containing sequence, d(ATGCAT)$_2$, and to compare these structural properties with those described previously for the chromomycin–d(ATGCAT)$_2$ complex (Banville et al., 1990).

Materials and Methods

Mithramycin A, produced by *Streptomyces plicatus*, was purchased from Sigma (St. Louis, MO) and used without further purification. The self-complementary oligonucleotide hexamer d(ATGCAT)$_2$ was purchased from Pharmacia. On the basis of its ^{1}H NMR spectrum, no further purification was necessary.

The NMR sample of d(ATGCAT)$_2$, 4 mM in duplex, was made by dissolving the hexamer in borate buffer (0.10 M borate, 0.18 M NaCl, 20 mM $MgCl_2$, pH 8.1) or phosphate buffer (20 mM sodium phosphate, 0.18 M NaCl, 20 mM Mg^{2+}, pH 8.1) and lyophilizing three times with D_2O (Aldrich, 99.96%). A stock solution of mithramycin was prepared by dissolving the solid in deionized water, and undissolved drug was removed by filtration. Its concentration was determined by visible spectroscopy with an extinction coefficient of 13 000 $M^{-1}\cdot cm^{-1}$ at 404 nm (in a 1 M NaCl, 100 mM borate buffer, pH 8.0, at room temperature). The mithramycin–DNA complex was formed by lyophilizing aliquots of the drug and adding hexamer solution to each aliquot. The final 0.4-mL sample for two-dimensional NMR contained either 100% D_2O or 10% D_2O/90% H_2O. The duplex concentration was determined by UV spectroscopy as described earlier (Banville et al., 1990).

All ^{1}H spectra were collected on a General Electric GN-500 NMR spectrometer operating at a proton frequency of 500 MHz and processed on the Sun/AT&T System 4 computer with software developed at UCSF. Two-dimensional phase-sensitive NOESY data (200- and 400-ms mixing times) were acquired in the pure absorption mode by the method of States et al. (1982) with 2K data points in the t_2 dimension and 400 data points in the t_1 dimension. At least 16 scans per t_1 increment were acquired. The bandwidth was about 5000 Hz with a recycle delay of 5.4 s and a presaturation pulse on the residual HOD signal. In general, apodization was carried out with Gaussian window functions and zero filling once in each of the two dimensions to yield a 4K by 1K map. All ^{1}H chemical shifts were referenced to the HOD signal at 4.89 ppm. A NOESY spectrum was obtained on a sample containing 90% H_2O with a modified selective $1\bar{3}\bar{3}\bar{1}$ pulse, a 80-μs pulse delay, a 5-s repetition time, and a 12 048-Hz bandwidth. The data were processed as described above.

Homonuclear correlation spectra (Aue et al., 1976; Neuhaus et al., 1985) were obtained with the double quantum filtered COSY experiment in the pure absorption mode and with the time-proportioned phase incrementation method (Redfield & Kuntz, 1975; Bodenhausen et al., 1980; Marion & Wuthrich, 1983). The data were collected with 2K data points in t_2 and 800 data points in t_1 and zero filled once in each dimension after apodization with a Gaussian window function. A modified two-dimensional homonuclear Hartmann–Hahn relay experiment (HOHAHA; Hartmann & Hahn, 1962; Davis & Bax, 1985) was performed with the MLEV-17 spin-lock pulse (Bax & Davis, 1985) with an Astron RS-4A amplifier and a 90° pulse of 37 μs. A total of 4K data points in t_2 and 400 data points in t_1 were collected, zero filled once, and apodized by a Gaussian window function in both dimensions.

Results

^{1}H NMR Assignments of d(ATGCAT)$_2$ in the 2:1 Complex of Mithramycin-d(ATGCAT)$_2$

Nonlabile Proton Assignments. Assignment of the d(ATGCAT)$_2$ protons in the drug–DNA complex were made from NOESY and COSY experiments. The results are summarized in Table I and compared with those previously obtained for drug-free d(ATGCAT)$_2$ under identical salt and temperature conditions (Banville et al., 1990). Each nucleotide is referred to by its 5′- to 3′-position in the duplex, i.e., A1, T2, G3, C4, A5, and T6. At the molar ratio (R) of one mithramycin per duplex of d(ATGCAT)$_2$, two sets of H1′ to H8 or H6 connectivities were mapped, and one set corresponds to the drug-free duplex while the other corresponds to the drug-bound duplex (Figure 2A). Assignments for the drug-free duplex were confirmed by comparison of both the chemical shifts and NOESY cross-peaks with those of the d(ATGCAT)$_2$ hexamer alone. At R = 2 (drug molecules per duplex), free DNA signals are absent, and only the set of drug-bound H1′ to H8,H6 signals is found (Figure 2B). Similar to the drug-free spectrum, the drug-bound spectrum

Table I: Proton Chemical Shift Assignments of $d(ATGCAT)_2$ and Mithramycin in the R = 2.0 Complex[a]

DNA protons	bound	free − bound MRA	free − bound CRA	MRA protons	bound	free − bound
A1H8	8.25	−0.07	−0.20	mr2	4.54	+0.24
A1H2	8.00	−0.06	−0.17	mr3	2.88	−0.06
A1H1′	6.17	+0.04	−0.01	mr4a	2.82	+0.15
A1H2′	2.67	+0.02	−0.19	mr4e	2.64	+0.01
A1H2″	2.87	+0.02	−0.01	mr7	2.68	−0.55
A1H3′	4.87	+0.01	+0.01	mr5	6.92	−0.05
A1H4′	4.24	+0.05	+0.09	mr10	6.67	+0.18
A1H5′,5″	3.84			mrOH	16.05	−0.10
T2H6	7.39	−0.03	−0.27	mr1′	5.03	−0.19
$T2CH_3$	1.35	+0.03	−0.04	mr3′,4′	4.30	−0.04
T2H1′	6.03	−0.29	−0.51	mr5′	1.35	−0.05
T2H2′	2.25	−0.06	−0.68	mr1′OMe	3.47	−0.03
T2H2″	2.69	−0.23	+0.03	1A	5.47	−0.16
T2H3′	4.96	−0.04	+0.00	2aA	2.13	−0.31
T2H4′	4.33	−0.09	−0.06	2eA	2.98	−0.60
T2H5′,5″	4.21			3A	4.19	−0.49
T2NH3	13.80			4A	3.34	−0.11
G3H8	7.70	+0.23	+0.31	5A	3.77	−0.14
G3H1′	6.12	−0.18	−0.03	6MeA	1.50	−0.24
G3H2′ or 2″	2.82	−0.17 or −0.02	−0.12	1B	5.15	−0.45
G3H2″ or 2′	2.67	+0.05 or −0.10	+0.15	2aB	1.71	−0.10
G3H3′	4.86	+0.16	+0.62	2eB	2.31	−0.13
G3H4′	4.33	+0.09	+0.39	3B	3.73	−0.15
G3H5′	4.22			4B	3.13	−0.15
G3H5″	4.43			5B	3.73	−0.43
G3NH1	12.52	+0.21		6MeB	1.37	−0.07
G3NH2(w)	7.33	−0.15		1C	4.74	+0.37
G3NH2(n)	5.78	+0.04		2aC	1.93	−0.33
C4H6	7.19	+0.19	+0.24	2eC	2.46	+0.07
C4H5	5.20	+0.22	+0.18	3C	2.12	+1.54
C4H1′	5.50	+0.19	+0.16	4C	3.06	−0.03
C4H2′	1.84	+0.18	−0.11	5C	2.98	+0.51
C4H2″	1.58	+0.83	+0.59	6MeC	1.36	−0.08
C4H3′	4.33	+0.54	+0.60	1D	2.64	+2.05
C4NH4(w)	8.28	−0.15		2aD	1.43	+0.35
C4NH4(n)	6.68	+0.04		2eD	1.87	+0.07
A5H8	8.30	+0.04	+0.12	3D	3.64	+0.25
A5H2	8.14	−0.27	−0.32	4D	3.84	−0.89
A5H1′	6.73	−0.41	−0.46	5D	3.50	−0.12
A5H2′	2.66	+0.11	−0.07	6MeD	1.25	+0.05
A5H2″	2.90	+0.01	+0.07	1E	5.40	−0.44
A5H3′	4.96	+0.08	+0.11	2aE	1.78	−0.24
A5H4′	4.83	−0.39	−0.40	2eE	2.23	−0.35
A5H5′ or 5″	3.33			3MeE	1.43	−0.22
A5H5″ or 5′	4.32			4E	3.16	−0.22
T6H6	7.34	−0.06	−0.16	5E	4.06	−0.42
$T6CH_3$	1.46	+0.07	+0.10	6MeE	1.50	−0.28
T6H1′	6.23	−0.10	−0.17			
T6H2′	2.17	+0.01	−0.24			
T6H2″	2.17	+0.01	−0.01			
T6H3′	4.58	−0.03	−0.05			
T6H4′	3.96	+0.08	+0.01			
T6H5′ or 5″	4.04					
T6H5″ or 5′	4.22					
T6NH3	13.45					

[a] Deviations between the drug-free and drug-bound DNA resonances are reported for the mithramycin and chromomycin complexes of $d(ATGCAT)_2$. Deviations between drugs bound to the DNA duplex in water and free in organic solvent, deuterated acetone for mithramycin and chloroform for chromomycin (Thiem & Meyer, 1981, 1979), are also reported. Shifts are given relative to the HOD reference at 4.89 ppm for aqueous solutions and relative to the $Si(CH_3)_4$ reference at 0 ppm for the organic solution.

is indicative of a C_2 symmetric hexamer complex.

The geminal H2′,2″ ^{1}H chemical shifts were distinguished by their relative cross-peak intensities with H1′ and confirmed by their intensities with H8 or H6. It was not possible to use the double quantum filtered COSY data for this purpose due to increased line broadening (about 12 Hz) caused by the bound drug. On the basis of the NOESY data, the C4H2″ chemical shift is upfield of that of C4H2′. This is unusual with respect to the results expected and obtained for the drug-free hexamer where H2″ is typically downfield of H2′ (Banville et al., 1990). It was not possible to distinguish

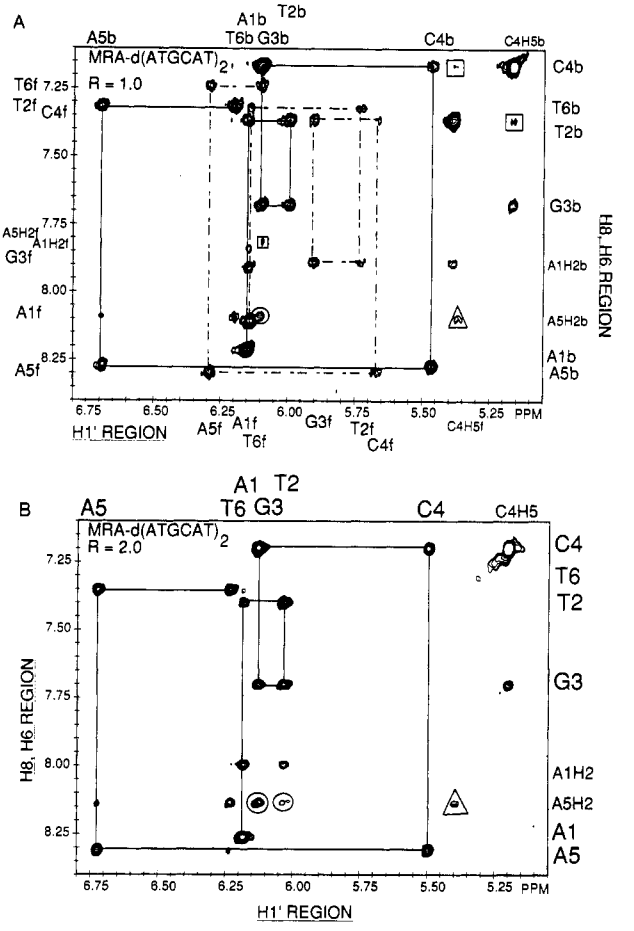

FIGURE 2: The H1′ to H8,H6 connectivities are traced for the NOESY region of $d(ATGCAT)_2$ complexed with mithramycin at a 200-ms mixing time and 15 °C. The hexamer sample was prepared in buffer containing 20 mM magnesium chloride. The DNA solution contains (A) 1 molar equiv of mithramycin per duplex (R = 1, in borate buffer) or (B) 2 molar equiv of mithramycin per duplex (R = 2, in phosphate buffer). Proton assignments of the drug-free hexamer (f) and the drug-bound hexamer (b) are indicated along the vertical (H8,H6) and horizontal (H1′) axes. The triangles indicate drug–DNA contacts, the circles cross-strand contacts, and the squares chemical exchange cross-peaks.

between the geminal protons of G3 due to overlap with other cross-peaks. Chromomycin had a similar effect—reversing the relative chemical shifts of the C4 geminal protons. In addition, chromomycin reversed the order of the T2 and G3 geminal protons.

Spin coupling between H4′, H5′, and H5″ was observed in the COSY data for A1 and T2 and confirmed by NOESY data. From HOHAHA data, spin coupling from G3H4′ to both G3H5′ and G3H5″ resonances (4.21 and 4.43 ppm) was observed. This was confirmed in the NOESY spectrum and the COSY spectrum where G3H5′ and G3H5″ appear strongly coupled. On the basis of the predictably stronger cross-peak intensity T2H1′ shares with the G3H5′ resonance and assuming a B-DNA conformation, the 4.21 and 4.43 ppm resonances are specifically assigned to H5′ and H5″, respectively. A5H4′ and T6H4′ do not show coupling to the respective H5′ and H5″ protons in the COSY spectrum, although coupling is found between the H5′ and H5″ protons. In these two latter cases, NOESY data were needed to confirm these geminal proton assignments. Extensive cross-peak overlap prohibited distinguishing between each of the two geminal H5′,5″ protons.

Difficulties in assigning the C4H4′, C4H5′, and C4H5″ resonances for this drug–DNA complex are very similar to

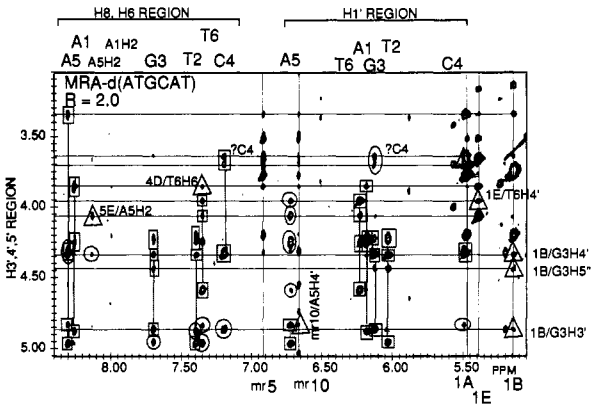

FIGURE 3: A region in the 200-ms NOESY map of the $R = 2$ sample at 15 °C and in phosphate buffer. DNA *intra*nucleotide contacts are indicated by squares while the *inter*nucleotide contacts are circled. Although the H3',H4',H5' region of DNA overlaps extensively with the mithramycin protons, several drug to DNA contacts are resolved and indicated by triangles. The tentatively assigned C4H4' and/or C4H5' protons at 3.64 and 3.68 ppm have contacts with C4H6 and G3H1' and potentially C4H1' and 1A as shown on this plot (see the text for details).

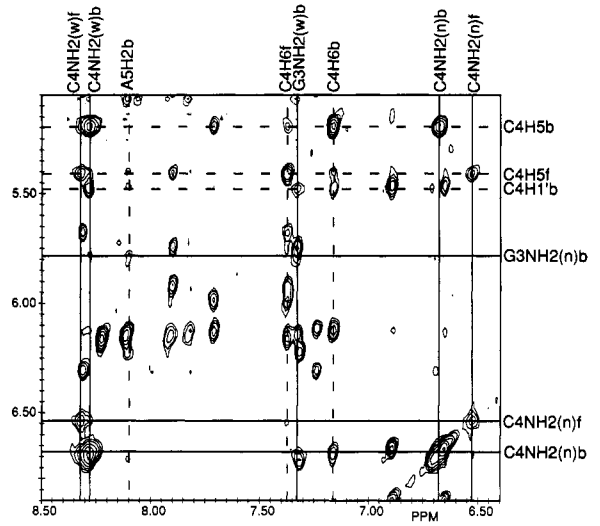

FIGURE 4: Amino proton NOE contacts in the aromatic to H1' region are shown for the $R = 1$ sample at a mixing time of 400 ms (90% H_2O/10% D_2O, borate buffer, 15 °C). The solid lines indicate contacts between labile protons, while the dashed lines indicate contacts between labile and nonlabile protons.

those observed in our previous study with chromomycin (Banville et al., 1990). Spin coupling among the H3', H4', H5', and H5" protons is not observed in the COSY data. On the basis of NOESY data, the unassigned resonances at 3.64 and 3.68 ppm could be assigned to the H4', H5', and/or H5" protons. Alternatively, the H4' and H3' resonances may overlap, leaving the 3.54 and 3.68 ppm resonances assignable exclusively to the two H5' protons. These two resonances show NOE contacts to C4H3', C4H6, G3H1', and each other (Figure 3). Although strong NOE contacts to C4H1' are possible, these two cross-peaks are sufficiently broad to be interpreted as contacts to both the C4H1' and the drug 1A resonances (Figure 3). This is consistent with the drug–DNA contacts described below.

Labile Proton Assignments. Most of the drug-free and drug-bound amino proton (NH_2) resonances were assigned from a 90% H_2O NOESY experiment with the $R = 1$ sample (see Figure 4). The two C4NH_2 protons were assigned by their strong NOE contacts to each other and to the C4H5 proton. Both drug-bound and drug-free Watson–Crick protons

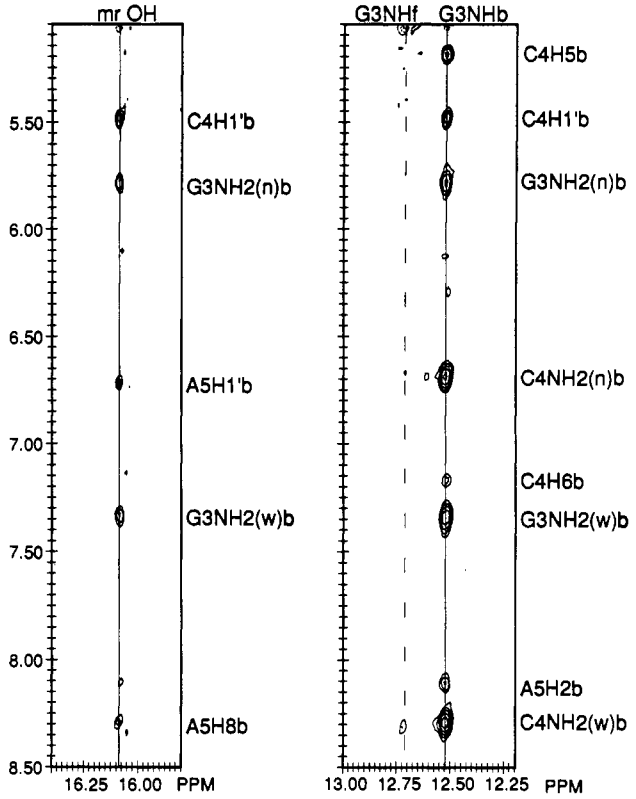

FIGURE 5: NOESY map at a 400-ms mixing time for $R = 1$ (90% H_2O/10% D_2O, borate buffer, 15 °C) shows NOE contacts from the bound DNA G3 imino proton (G3NHb) and the drug phenolic proton (mrOH) to several DNA protons.

resonate downfield from their non-Watson–Crick protons. The two G3NH_2 protons are usually degenerate due to rapid rotations about the carbon–nitrogen bond (Banville et al., 1986). However, this does not appear to be the case for the 2:1 complex where resonances assignable to the Watson–Crick (w) and non-Watson–Crick (n) G3NH_2 protons are identified at 7.33 and 5.78 ppm, respectively. Other NOE contacts from G3NH_2(n) to both A5H2 and C4NH_2(w) and from G3NH_2(w) to C4H1' support these assignments. The G3NH_2 resonance of drug-free DNA does not appear in the aromatic to H1' region and has not been assigned.

As shown in Figure 5, the bound G3 imino proton (G3NH) has NOE contacts to several nearby amino protons (both G3NH_2 protons, both C4NH_2 protons) and to nonlabile C4 and A5 protons (C4H5, C4H1', C4H6, and A5H2). The relative intensities of these cross-peaks are consistent with the long mixing time used (400 ms). NOE contacts involving all of the thymine imino protons and the guanine drug-free imino proton are in general too weak to observe. This must reflect differences in chemical exchange with the solvent.

Conformational Analysis of d(ATGCAT)$_2$ in the 2:1 Complex

Tables II and III summarize the DNA intranucleotide and internucleotide NOESY contacts for the mithramycin–d-(ATGCAT)$_2$ complex. Both the presence and absence of NOE cross-peaks and the relative intensities of these cross-peaks are used to evaluate sugar pucker and the overall conformation of the helix (Arnott & Hukins, 1972; Wuthrich, 1986).

NOE Contacts between T2/T2 and T2/G3. Prominent cross-peaks are observed at 200 ms for T2 between Me/H2' and Me/H3' of the 2:1 complex. For the drug-free duplex, these same cross-peaks are not observed or are too weak to measure. This suggests that the T2Me portion of the base is placed closer to its deoxyribose protons in the 2:1 complex.

Table II: 200-ms NOESY Cross-Peak Intensities of the Intranucleotide Contacts within d(ATGCAT)$_2$ in the 2:1 Complexes of MRA (Lower Left Diagonal) and CRA (Upper Right Diagonal)

A1	H8	H2	H1'	H2'	H2"	H3'	H4'	H5'=H5"
H8			m	m	m	m	w	ov
H2			m					
H1'	m	w		s	s	m	m	
H2'	m	w	m		s		m	
H2"	m	w	s	ov			m	
H3'	w		w	ov	m		m	
H4'	w		ov	ov	m	m		
H5'‖H5"	m		w			m	s	

T2	H6	Me	H1'	H2'	H2"	H3'	H4'	H5'	H5"
H6		s	ov	ov	ov	ov	m		
Me	s		w	m		ov	ov		
H1'	m	w		s	s	m	m		
H2'	s	m	m		s	s	ov		
H2"	ov	m	s	s		m	ov		
H3'	m	m	m	m	ov		s		
H4'	w	ov	m	w	ov	m			
H5'‖H5"	m		ov	w	ov	s	s		

G3	H8	H1'	H2'	H2"	H3'	H4'	H5'	H5"
H8		m	ov	m	m	m		
H1'	m		m	m	m	m		
H2'	m	s		s	ov			
H2"	ov	ov	ov		ov	ov		
H3'	m	m	m	ov		m		
H4'	w	m	ov	ov	m			
H5'	w	w		ov	m	ov		
H5"	w	w		w	m	m	s	

C4	H6	H5	H1'	H2'	H2"	H3'	H4'	H5'	H5"
H6		s	m			m			
H5	s								
H1'	w	w		s	s	m			
H2'	w		s		s	m			
H2"	w		s	m		m			
H3'	m	w	m	m	m		ov		
H4'									
3.68	w		m			w			
3.64	w		w			w		ov	

A5	H8	H2	H1'	H2'=H2"	H3'	H4'	H5'	H5"
H8		ov	m	m	m			
H2			m					
H1'	m	w		m	m	m		
H2'	m		m					
H2"	m		s	ov		s	m	
H3'	m		m	ov	m			
H4'	w		w		m	ov		
H5'	w				m	m		
H5"	ov				m	m	s	

T6	H6	Me	H1'	H2' = H2"	H3'	H4'	H5'	H5"
H6		s	m	s	m	ov		
Me	s			m				
H1'	m	ov		s	m	m		
H2'‖H2"	s	ov	ov		s	m		
H3'	m	w	m	s		m		
H4'	w		m	m	m			
H5'	w		w	m	m	m		
H5"	w		w	m	m	m	s	

The internucleotide contacts from G3H8 to several T2 protons (H6, Me, H2′, H2″, and H3′) support this conclusion. By comparison, the hexamer alone shows no G3H8 contacts to T2Me of T2H3′ and weaker contacts to T2H2′ and T2H2″. One explanation is that a tilt in the plane of the T2 and G3 bases is induced by mithramycin binding such that the major groove portion of T2 and G3 is brought closer together while the minor groove portion is pulled further apart. Drug-mediated spin diffusion between these DNA protons does not seem likely given the predominantly minor groove binding character of the drug and the fact that there are no single drug protons between T2 and G3 (see Discussion).

NOE Contacts between G3/C4 and G3/A5. For the complex, G3H8 has essentially identical NOE cross-peak intensities with C4H6 and C4H5. This is not expected for the standard B-DNA conformation of d(ATGCAT)$_2$ where the G3H8 to C4H5 cross-peak intensity is about twice that of the G3H8 to C4H6 intensity. Two additional observations argue in support of a change surrounding the GC basis. First, there are several cross-strand NOE contacts from G3 (H1′, H2′, H2″, H4′) to A5H2 for the 2:1 complex, while similar contacts are not measurable for D(ATGCAT)$_2$ alone. On the basis of comparisons with A-form DNA, this indicates a widening of the minor groove. Drug-mediated spin diffusion from the drug phenol proton to A5H2 and G3H1′ could also contribute to the increased intensity of these DNA cross-peaks. Second, both C4H6 and C4H5 have significantly stronger NOE contacts to G3H1′, G3H2′ and G3H2″ for the drug-bound form of d(ATGCAT)$_2$. On the basis of the absence of NOE contacts from the drug protons to G3H1′, G3H2′, and G3H2″, it is not likely that the presence of the drug has mediated spin diffusion between these DNA protons. Hence, the stacked GC bases are apparently altered by drug binding.

Internucleotide H8,H6 to H1′,H2′,H2″ Cross-Peaks. For the drug–DNA complex, the NOE cross-peak intensities from A5H8 to C4H2′ are stronger than those to C4H2″ and C4H1′. This is contrary to the drug-free hexamer where the A5H8 to C4H2′ cross-peak has the weakest intensity of the three contacts. Other internucleotide contacts do not show as significant a difference in cross-peak intensities. Thus, mithramycin appears to alter the base stacking of C4-A5 or the sugar pucker of C4.

A5H1′ to H2′,H2″. A predominantly C2′-endo sugar pucker is marked by large intensity differences between the H1′/H2′

Table III: 200-ms NOESY Cross-Peak Intensities of the Internucleotide Contacts within d(ATGCAT)$_2$

MRA-d(ATGCAT)$_2$

T2 \ A1	H8	H2	H1'	H2'	H2"	H3'	H4'	H5'	H5"
H6	w		w	ov	m	m			
H7	m	w	w			m			
H1'		w							
H4'			w						
H5'= H5"			m						

G3 \ T2	H6	Me	H1'	H2'	H2"	H3'	H4'	H5'	H5"
H8	w	w	m	m	ov	w			
H5'			ov						
H5"			w						

C4 \ G3	H8	H1'	H2' or 2"	H2" or 2'	H3	H4'	H5'	H5"
H6	w	m	m	s	m			
H5	w	w	m	m	w			
H1'		w	w	m				
3.68		w						
3.64		w						

A5 \ C4	H6	H5	H1'	H2'	H2"	H3'	(H4'	H5' 3.68	H5") 3.64
H8	w		m	s	m	ov			
H2			w						
H4'			w						

T6 \ A5	H8	H2	H1'	H2'	H2"	H3'	H4'	H5'	H5"
H6	w		m	m	m	m	w		
H7	m		m		m	m			
H1'	w		w						
H2'= H2"			w						
H3'			w						
H4'			w						
H5' or 5"			w						
H5" or 5'			m						

CRA-d(ATGCAT)$_2$

T2 \ A1	H8	H2	H1'	H2'	H2"	H3'	H4'	H5' = H5"
H6			w		ov	m	m	
H7	m	w	w			s		
H1'		w						
H4'								
H5'= H5"								

G3 \ T2	H6	Me	H1'	H2'	H2"	H3'	H4'	H5'	H5"
H8	ov	ov	ov	ov	ov				
H5'									
H5"									

C4 \ G3	H8	H1'	H2'	H2"	H3'	H4'	H5'	H5"
H6	w	m	m	m	m	w		
H5	w	w	m					
H1'								
H5'								
H5"								

A5 \ C4	H6	H5	H1'	H2'	H2"	H3'	H4'	H5'	H5"
H8			m	s	m	m			
H2									
H4'									

T6 \ A5	H8	H2	H1'	H2'=H2"	H3'	H4'	H5'	H5"
H6			w	m	m			
H7	m		w	m	s			
H1'		m						
H2'= H2"								
H3'								
H4'								
H5'								
H5"								

and H1′/H2″ cross-peaks, and this is observed for A1, T2 and C4 (G3 and T6 could not evaluated due to overlap). However, A5 has a small intensity difference that is about one-sixth of the difference observed for drug-free d(ATGCAT)$_2$. Some significant drug-induced changes could occur in the deoxyribose pucker of A5. A similar comparison with the chromomycin–dNATGCAT)$_2$ complex is not possible due to chemical shift overlap of A5H2′ and A5H2″.

Intranucleotide H8,H6 to H2′,H2″,H3′ Cross-Peaks. Small intensity differences between the H8,H6 to H2′ and H2″ cross-peaks are noted for C4 and A5 of the 2:1 complex but not for the drug-free hexamer. This strongly suggests that the average orientation of each base with respect to its sugar is altered in the complex. Further confirmation comes from a significant enhancement of the H8,H6 to H3′ cross-peak intensities for the drug complex. Enhancements of greater than 75% are particularly noted for C4 and T2 and add further support ot the assertion that mithramycin induces a change in the orientation of the base relative to the sugar for these residues.

Chemical Shift Deviations. As shown in Table I, the largest chemical shift deviations of DNA protons occurs in the central four base pairs, i.e., -TGCA-. The largest of the upfield chemical shift occurs at C4H2″ and C4H3′ with deviations of +0.83 and +0.54 ppm, respectively. Furthermore, the remaining nonlabile cytosine protons are also consistently shifted upfield by about 0.2 ppm. In contrast, the neighboring nucleotide, G3, has a mix of upfield and downfield chemical shift deviations which range from 0.1 to 0.2 ppm. The largest downfield shift is at A5H1′ with a deviation of −0.41 ppm. A similarly significant downfield shift at the minor groove proton A5H2 is contrasted by a negligible change in the major groove proton A5H8.

In most cases the chromomycin and mithramycin chemical shift deviations are comparable. For example, G3 and C4 aromatic proton chemical shifts are similar for the two drug complexes. However, the aromatic protons A1, T2, and T6 are shifted much more downfield in the chromomycin complex than in the mithramycin complex with the exception of T2 and T6CH$_3$. Hence, some structural differences near the ends of

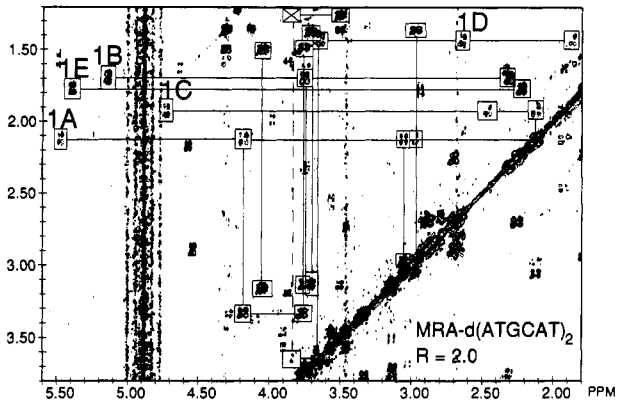

FIGURE 6: Double quantum filtered COSY data showing the *J* coupling connectivities among each of the mithramycin hexapyranose protons for the 2:1 complex (phosphate buffer, 15 °C).

$d(ATGCAT)_2$ may be presumed between the two drug complexes.

^1H NMR Assignments of Mithramycin in the 2:1 Complex of Mithramycin-$d(ATGCAT)_2$

NOESY, COSY, and HOHAHA data were necessary to assign most of the mithramycin ^1H chemical shifts. These are summarized in Table I. Figure 6 shows spin coupling within the A-, B-, C-, D-, and E-hexapyranoses of mithramycin. The A- and B-hexose spin systems can be completely traced out in the COSY map. They are distinguishable from one another by the strong NOE contacts of A-hexose spin system has with the chromophore proton mr5.

As expected for the E-hexapyranose, the proton connectivity is broken at carbon 3 but resumes from 4E to 6MeE. Both NOESY and HOHAHA data confirm these hexapyranose assignments. Several NOE contacts between the C-hexose and m2 are expected in the 200-ms NOESY map. Of the 11 NOE contacts to m2, 5 previously unassigned contacts can be attributed to the C-ring: 4.74, 3.06, 2.98, 2.46, and 1.93 ppm. First, 1C is assigned to the 4.74 ppm resonance on the basis of the very strong cross-peak it makes with m2 and the generally downfield placement of this hexose proton. Spin coupling can be traced the entire C-ring, allowing for the subsequent assignment of all seven C-hexose protons (Table I; Figure 6). Mutual NOE contacts between all seven protons except 2aC to 6MeC are observed at the 200-ms mixing time.

Spin coupling about the D-hexose ring was not complete; hence, the assignment of these protons was made last. A strong NOE between the 3C and 2.64 ppm resonance indicated that 1D resonated unusually upfield at 2.64 ppm. Spin coupling could be traced from this 1D resonance to 4D and from 5D to 6MeD. No coupling between 4D and 5D was observed. At mixing time of 200 ms, it was possible to observe NOE contacts between each of the D protons with the exception of 6MeD contacts to the geminal 2D protons. As expected, several cross-peaks from the D-ring to 3C and 1E were clearly observed.

The chromophore methyl (mr7) was not easily assigned due to overlap with the G3H2″ or G3H2′ resonance at 2.68 ppm. Nevertheless, the narrow line widths of several cross-peaks, e.g., mr7 with 1E and 5E, associated with this resonance are attributes typical of uncoupled methyl protons and not of DNA sugar protons.

The aliphatic ring protons were assigned from the COSY spectrum and confirmed in the NOESY spectrum. A strong COSY cross-peak between mr2 and mr3 suggested that these protons are in an axial position. No spin coupling was observed for the aliphatic ring proton mr3 to the side-chain proton H1′. The mr1′ resonance is assigned to 5.03 ppm on the basis of a strong NOE cross-peak with mr3. Strong spin coupling between m5′ and mr4′ protons and NOE contacts, e.g., mr1′ to mr3 and mr4′ to m5′, are consistent with these side-chain protons assignments. From the intensity and shape of the NOESY cross-peaks with mr4′ it is apparent that the mr3′ and mr4′ resonances overlap.

The 90% H_2O/10% D_2O NOESY revealed at least one prominent phenolic proton at 16.05 ppm. This roughly corresponds to the phenolic proton mr9OH in acetone (Thiem & Meyer, 1981). Until mr9OH can be clearly differentiated from its neighboring phenolic proton, mr8OH, we will refer to the 16 ppm resonance as mrOH. A weaker and broader resonance at 15.8 ppm is also observed (see below). Due to the lack of NOE contacts between this 15.8 ppm resonance and other mithramycin protons, this resonance has not been assigned.

Conformational Analysis of Mithramycin in the 2:1 Complex

Side Chain and Chromomycinone Ring. The chromophore ring and aliphatic side chain of chromomycinone have several prominent intramolecular NOE contacts (e.g., mr5/mr10, mr2/mr3, mr3/mr4a, mr3/mr4e, and among the aliphatic protons). Contacts between the ring and the side chain are also observed (mr10 to mr1′, mr3′,4′, and mr1′OMe; mr5 to mr1′OMe; mr4a to mr1′OMe and mr1′; mr3 to mr1′OMe; mr2 to mr1′, mr3′,4′, and mr1′OMe).

A- and B-Hexapyranose Contacts. At the 200-ms mixing time, the A- and B-hexapyranoses have an extensive number of contacts within each ring. In addition 1B shows several contacts to the A-ring with the most prominent one involving 3A and 1B. These contacts are consistent with weaker contacts from 3A to 3B,5B. Moderately strong contacts from 3A to 5B,2eA and from 2aA to 1B are also observed.

The A-hexapyranose has a large number of contacts to the chromophore ring. The strongest contact from mr5 to 1A and 5A places the A-ring very close to the hydrophobic edge of chromomycinone. Several contacts from the A-hexapyranose to the D-hexapyranose, however, suggest the possibility of intermolecular drug contacts within the drug dimer. A particularly strong cross-peak between 6MeA and 4D is supported by more moderate contacts from 1A to 1D, 5D, and 6MeD and from 5A to 3D. A weaker cross-peak from 4A to 1E is also observed.

D- and E-Hexapyranose Contacts. The 1E and 5E protons show several NOE contacts to the D-hexose ring. The strongest contact is from 1E to 3D. Moderate contacts from 1E to 4D and from 5E to 4D and several other contacts are consistent with these stronger D to E contacts. Several possible contacts between two drug molecules are observed from the E- and D-rings of one drug to the chromophore methyl protons, mr7 and mr5, of the other drug. The stronger contacts are from mr7 to 1E and 5E; these are followed by more moderate contacts from mr5 to 5D, 6D, and 4D. The mr5 to D-ring contacts are consistent with weaker contacts to mr10. Very weak contacts from 1E to mr5 and from mr7 to 2eD and 4D are also observed and fully consistent with these D- and E-ring contacts to the chromophore. Thus, the relative positions of the D- and E-rings are such that the D-ring is closer to the mr5 proton and the E-ring is closer to the mr7 methyl protons. These D- and E-hexose contacts to the chromophore are more likely interdrug contacts on the basis of the strong coupling between mr2 and mr3 which places these protons in a more diaxial position to one another, thereby shifting the CDE-chain away from its own chromophore ring. Similar results were

found for the chromomycin complex with d(ATGCAT)$_2$ and d(TTGGCCAA)$_2$ (Banville et al., 1990; Gao & Patel, 1989a).

C- and D-Hexapyranose Contacts. The 1C proton has a strong NOE contact with the nearby chromomycinone mr2 proton and progressively weaker contacts to mr3 and mr4e. A moderate contact from 1C to the side-chain proton, 1′OMe, places this functional group in the vicinity of the C-hexose ring. Contacts to the 1D and 3D protons are observed as well. A particularly strong contact between 3C and 1D is supported by moderate contacts to 3D, 6MeD, and 5D and a weak contact from 2eC to 1D.

Chemical Shift Deviations of Mithramycin. Due to the insolubility of mithramycin in water in the absence of DNA and magnesium, it was not possible to obtain the chemical shift values of unbound mithramycin. Hence, chemical shift deviations of the mithramycin protons in the DNA complex are compared with the values Thiem and Meyer (1981) reported for mithramycin in acetone. These results are summarized in Table I.

The aliphatic chain protons H3′,4′ and H5′ have small changes in chemical shift. However, large deviations are observed in the remainder of the molecule. Particularly noteworthy are the large upfield shifts in 3C and 1D of +1.54 and +2.05 ppm, respectively. Large upfield shifts of this magnitude can be induced by ring current effects from the nearby aromatic portion of the chromomycinone ring system. Similar results were first reported by Gao and Patel (1989a).

Other large deviations in chemical shift are most likely due to interactions between the drug and the DNA and to the conformational differences of mithramycin in an aqueous versus a nonaqueous environment. For example, the E-hexose ring, which has an extensive number of drug–DNA contacts, also has downfield proton shifts of more than 0.2 ppm. Downfield shifts ranging between 0.1 and 0.6 ppm are also observed for both the A- and B-hexose rings. The largest shift for the chromophore involves a −0.55 ppm shift in the methyl functional group, mr7.

NOE Contacts between Mithramycin and d(ATGCAT)$_2$ in the 2:1 Complex

Upon reviewing Table IV, it is easy to see regional trends in the drug–DNA contacts of the nonlabile protons. In general, the E-hexapyranose has NOE contacts to minor groove protons (H2 of A5 and A1; H1′ of T2, 3, A5, and T6; Figures 2B and 3). D-Hexose contacts to the T6H4′ and T6H5″ and C-hexose contacts to A5H4′ and A5H1′ are observed. These contacts place the CDE carbohydrate chain away from the central GC base pairs. The AB carbohydrate chain has NOE contacts with the centrally located GC base pair protons. The A-ring has NOE contacts with both G3 (H3′, H4′, H5, H5″) and C4 (H6, H5′, H5″), while the B-ring contacts exclusively with G3 ribose protons (H3′, H4′, H5′, H5″). Some of these contacts are shown in Figure 3. The strongest C4 contacts are to 6MeA and 1A, and the strongest G3 contacts are to 5A and 6MeA. In comparison to the A-hexose contacts, the B-hexose contacts to G3 are weaker.

At least three nonlabile chromomycinone contacts from the mr7 methyl protons to G3H1′, a moderate contact from mr10 to the tentatively assigned C4H5″ proton, and a weaker contact from m10 to A5H4′ are observed. This positions the drug chromophore rings near the -GCA- portion of the hexamer. Relatively strong contacts from the labile hydroxyl group, mrOH, to both G3NH$_2$ protons, G3NH, and the H1′ of C4 and A5 (Figures 4 and 5) are consistent with this placement. A weaker contact to A5H8 is probably due to spin diffusion. For the same mixing times, a similar contact was seen in the 2:1 complex of chromomycin–d(ATGCAT)$_2$ but not seen at the shorter 50-ms mixing time.

Table IV: Mithramycin (MRA) and Chromomycin (CRA) Contacts with d(ATGCAT)$_2$ Observed in the 200-ms NOESY Spectrum[a]

DNA	MRA	CRA
A1H2	3MeE(s)	4E(w)
T2H1′	3MeE(m), 6MeE(w)	4E(m), 6MeE(m)
T2H4′		4fE(m)[c]
T2H5′[b]		4fE(w)
G3H8		4fA(m), 3B(u), 5B(u)
G3H1′	6MeE or 6MeA(w), m7(u)	cr7(s), 4fA(m)
G3H3′	5A(s), 1B(w)	
G3H4′	5A(m), 6MeA(s), 1B(m)	4A(w)
G3H5″	5A(s), 6MeA(m), 1B(m), 2eB(m)	
G3H5′	6MeA(u), 2eB(m)	
G3H5′[b] or C4H3′		4fA(s), 4B(u), 4fB(w)
C4H6	6MeA(m)	4fA(w), 4fB(w), 5D(w)
C4H1′		4fA(m), cr7(w)
C4H5′[b]	6MeA(s), 1A(s)	
C4H5″[b]	6MeA(s), 1A(s), m10(m)	
A5H2	1E(w), 2aE(w), 2eE(m), 3MeE(m), 5E(m), 6MeE(w), mr7(u)	1E(m), cr7(s), 2eD(w), 2eE(w), 2aE(w), 6MeE(m)
A5H1′	2aC(w), 2eC(w)	2aC(m)
A5H2′,2″		2eC(w)
A5H4′	1C(u), 2aC(s), 2eC(s), 4C(w), 1′OMe(u), m10(w)	2aC(m), 2eC(w)
T6H6	4D(w)	
T6H1′	1E(w), 2aE(m), 2eE(m), 3MeE(u)	1E(m), 2eE(s), 3MeE(w), 6MeE(w)
T6H4′	2aD(s), 2eD(s), 1E(m), 2aE(m)	1E(m), 2eE(m), 2aD(m)
T6H5″	2aD(s)	

[a] Relative cross-peak intensities are described as strong (s), medium (m), weak (w), or unresolved (u) from cross-peak overlap. [b] These assignments are tentative as described in the text. [c] f indicates the acetyl functional groups on the E- and A-hexapyranoses and the methoxyl functional group on the B-ring.

In addition to the 16.05 ppm resonance, a much weaker and broader resonance at 15.8 ppm is evident. The possibility of an impurity, excess drug, or a second type of drug–DNA complex cannot be eliminated. However, there is no doubling of the other drug or DNA peaks nor other easily identified impurity resonances. Another possibility is that this resonance is due to either the other phenolic or a hexapyranose hydroxyl. Yet, there are no NOE cross-peaks associated with the 15.8 ppm resonance.

Chemical Exchange

At R = 1.0, several off-diagonal cross-peaks which correspond to the drug-free and drug-bound duplex are observed in the aromatic and H1′ region. These cross-peaks are clearly absent at R = 2. Since a measure of the smallest chemical shift difference between the T2 methyl of free and complexed DNA is 15 Hz, the rate of chemical exchange is much slower than 15 s^{-1} (Dwek, 1973). Hence, this drug–DNA system is clearly in slow exchange on the NMR time scale yet fast enough to allow a transfer of magnetization between the free and bound states of DNA within the 200-ms mixing time.

Discussion

Mithramycin binds to d(ATGCAT)$_2$ to form a fully saturated complex by R = 2.0. As demonstrated by the similarity in cross-peaks for the bound duplex in Figure 2, an apparent stoichiometry of two drugs per one duplex is maintained at both molar ratios of one and two drugs per duplex. Furthermore, this stoichiometric 2:1 complex possesses an overall C_2 symmetry. These results are identical with those described previously for chromomycin binding to d(ATGCAT)$_2$ (Ban-

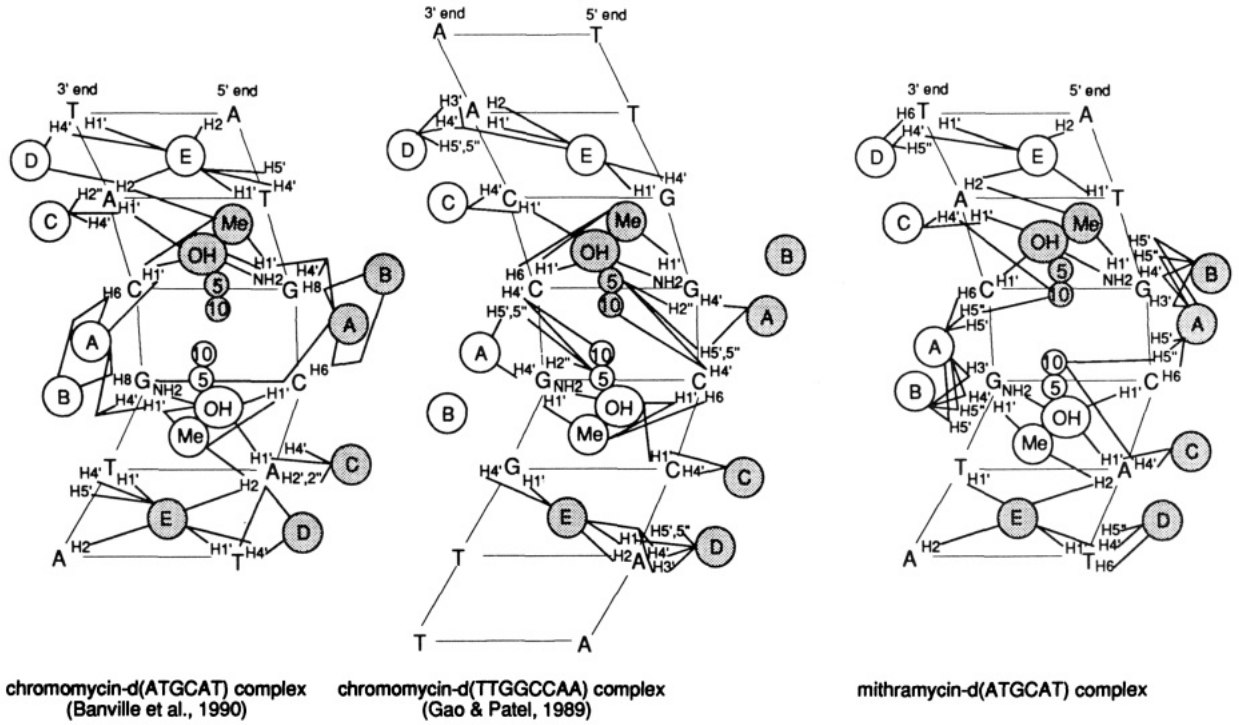

FIGURE 7: Summary of the 200-ms NOESY drug–DNA contacts studied to date. Selected regions of the drugs are shown as spheres, and the two drugs are differentiated by shading.

ville et al., 1990) and to d(TTGGCCAA)$_2$ (Gao & Patel, 1989a). Both mithramycin and chromomycin require at least one Mg^{2+} per duplex for complete binding to occur.

The mithramycin and chromomycin complexes formed with d(ATGCAT)$_2$ are in slow chemical exchange. This is proven at the R = 1.0 ratio where two separate sets of DNA resonances are observed and found to correspond to the free and bound forms of the DNA complex (Figure 2A). In the case of very slow exchange, chemical exchange cross-peaks are absent from the NOESY spectrum. This was found to be the case for the chromomycin complex but not for the mithramycin complex. Hence, mithramycin appears to be in slightly faster chemical exchange than chromomycin.

By assuming that the apparent binding constant of mithramycin to d(ATGCAT)$_2$ is high (ca. 10^6 M^{-1}; Brikenshtein et al., 1983; Prasad & Nayak, 1976), the rate of exchange is essentially a measure of the off-rate constant of the drug (Klevit et al., 1986). The 200-ms NOESY data can offer an upper limit of the off-rate constant of mithramycin from the ratio of the exchange cross-peak intensity to its diagonal cross-peak intensity. Several ratios were determined and found to be about 0.08. This means that 8 out of 100 drug dimers have dissociated in the 0.200-s mixing time. From the first-order rate equation, the off-rate constant is about 0.4 s^{-1}. Although this is an upper limit, when corrections are made for changes in magnetization due to T_1 relaxation (2–3 s) and chemical exchange, this value does not change significantly (Dwek, 1973).

Since chromomycin does not have easily identified chemical exchange cross-peaks at R = 1.0, the off-rate constant of chromomycin from d(ATGCAT)$_2$ is presumably much lower than 0.4 s^{-1}. Structural differences between these two drugs must account for the differences in exchange rate. Unlike mithramycin, chromomycin has acetyl groups on the A- and E-pyranoses and a methoxy group on the B-pyranose. These bulky groups can provide increased stabilization of the chromomycin–DNA complex through their interaction with water (Kam et al., 1988).

It is well-known that water stabilizes the structure of DNA (Alden & Kim, 1979). The phosphate electrostatic repulsion is diminished by the high dielectric constant of water and hydrated counterions. Binding of chromomycin and mithramycin requires that the hydrophilic portions of these hexapyranoses are similarly exposed to minimize both the drug–drug and drug–DNA repulsions of the phosphate, hydroxyl, acetyl, and methoxy groups. "Filaments" of water can connect and stitch together these anionic groups (Corongiu & Clementi, 1981). The hydrogen bonds that form these shells of hydration may have a significant stabilizing effect on the drug–DNA complex. The bulky acetyl groups on chromomycin are advantageous to binding. First, the acetyl groups have two oxygens instead of one. This increases the hydrophilicity of chromomycin. Second, the position of these oxygens can be redirected by rotation about the carbon–oxygen torsional angle connecting the acetyl to the hexose ring. This allows chromomycin to position the acetyl groups in the most advantageous position with respect to the DNA phosphate backbone. Hence, the lack of acetyl groups on mithramycin may acount for its faster off-rate from the d(ATGCAT)$_2$ duplex.

From the NOESY data a general model of the mithramycin–d(ATGCAT)$_2$ complex can be built and compared with the previous published models of chromomycin binding to d(ATGCAT)$_2$ and d(TTGGCCAA)$_2$. Figure 7 summarizes the drug–DNA contacts reported for each of these three complexes. The mithramycin complex has a remarkable similarity to those reported for chromomycin. The E-pyranose spans both strands of the DNA duplex, the chromophore is located near the requisite GC base pair, and the C-, D-, A-, and B-rings are skewed exclusively to one strand of the duplex. The most obvious difference in these three models is in the placement of the AB hexose chain.

The NOESY contacts between the A- and B-hexose rings of mithramycin and chromomycin differ. For mithramycin the strongest cross-peak contacts are 1B to 2aA and 1B to 2eA, and for chromomycin they are 1B to 4A and 1B to 3A. This

indicates that the relative orientation of the A- and B-rings differs for the two drugs. However, the A proton contacts to the chromophore ring are similar for both drugs, with strong NOE cross-peaks from 1A to the chromomycinone H5 and none to the methyl proton mr7. Thus the orientation of the A-ring is basically the same for both drug complexes. It is the orientation of the B-ring that appears to be the primary difference between these two drug complexes. Variations in ring pucker and in the torsional angle between A- and B-rings can account for these conformational differences. In the case of the mithramycin complex, the NOESY contacts indicate that the B-ring is closer to the A-ring, and this is consistent with the observed drug to DNA contacts.

Drug NOE contacts with the major groove protons of DNA demonstrate some of the differences in the orientation of the AB-chain about the two centrally located GC base pairs. Several protons on the B-ring of chromomycin and the acetyl group on the A-ring of chromomycin have contacts with G3H8. These contacts to a major groove proton of G3 are supported by several well-resolved contacts with the ribose protons of G3 (Table III; Figure 7). The A- and B-rings of mithramycin do not show similar contacts to G3H8 but do show a large number of contacts to the G3 ribose protons. Contacts from another major groove proton, C4H6, are observed to both the mithramycin and chromomycin AB-chains. For mithramycin there is only one cross-peak of medium intensity with the A-ring, 6MeA. The chromomycin complex has a larger variety of contacts from C4H6 to the 4A acetyl group, the 4B methoxy group, and 5D. All of these chromomycin contacts are very weak and appear to represent spin-diffusion contacts between drug and DNA. In contrast to these DNA hexamer complexes, the chromomycin–octamer complex has no NOE contacts to GH8 or CH6 (Gao & Patel, 1989; see Figure 7). Hence, these three complexes are basically similar in that their AB-chains are located between the -GC- bases but differ in their orientation about these bases.

Overall the position of the chromophore hydroxyl within the minor groove of ATGCAT appears to be the same for both drug complexes. Definitive contacts between each hydroxyl and the DNA protons (G3NH$_2$, C4H1′, and A5H1′) position this hydroxyl off center from the DNA helical axis of symmetry (see Figure 7; Figure 5). This is also true for the chromomycin–d(TTGGCCAA)$_2$ complex where hydroxyl contacts to G4NH$_2$, C5H1′, and C6H1′ were reported. Furthermore, NOE contacts from the chromophore methyl to GH1′ are similar for all three drug complexes (Figure 7). As described earlier, the hydrophilic edge of the chromophore appears to be pointed into the minor groove. In contrast, much weaker or poorly resolved contacts from the chromophore H5 and H10 to DNA protons are observed in all three cases. In the case of the chromomycin–hexamer complex, the aromatic H5 and H10 contacts to DNA are poorly resolved due to overlap and have been left undefined in Figure 7, while the mithramycin complex has at least one resolved drug to DNA contact and the chromomycin octamer complex has three. Therefore, the hydrophobic edge of both drug chromophores points out of the minor groove while the hydrophilic edge points inward. Furthermore, the relative positions of the H5 and H10 protons appear to be near the helical center of symmetry located between the two GC base pairs.

Similar to the chromophore hydroxyl, the E-hexose ring of mithramycin also has close contacts with the minor groove protons of d(ATGCAT)$_2$ (Figures 2B and 3). NOE contacts from the E-ring to T2H1′, A5H2, A1H2, and T6H1′ place this portion of mithramycin the furthest from the 2-fold axis of symmetry. This defines the drug dimer binding site as consisting of six consecutive base pairs.

Analogous contacts from the E-hexose of chromomycin to the minor groove protons of d(ATGCAT)$_2$, d(TATGCATA)$_2$, and d(TTGGCCAA)$_2$ are consistent with a six base pair binding site. This is comparable to footprinting studies carried out at approximately 100-fold lower drug concentrations, which indicate that three to four base pairs are protected at each drug binding site (Van Dyke & Dervan, 1983; Con & Fox, 1989). Although the drug spans six base pairs, the unprotected sugar–phosphate between A1 and T2 is the most likely location for cleavage in DNA footprinting (see Figure 7). This would yield a protected site of four base pairs plus two unpaired T2 bases:

TGCAT
TACGT

Thus, our NMR data and footprinting data are in agreement.

Subtle differences in the relative orientation of the E- and D-rings of mithramycin and chromomycin are found by comparison of their NOE intensities at the 200-ms mixing time. For mithramycin strong NOE contacts from 1E to 3D and 4D contrast with those of chromomycin from 1E to 2eD and 3D. Some of these disparities can be due to structural differences inherent in the E-rings of both drugs (Figure 1). Similarities are found between the position of the E-ring and the neighboring chromophore ring. The 1E proton of both drugs has strong contacts with the chromophore methyl, mr7. On the basis of the chromomycin model proposed earlier and shown in Figure 7, this is an intermolecular drug contact (Banville et al., 1990; Gao & Patel, 1989a). Other intermolecular contacts involving the D-hexose ring are found to be consistent with this model.

Intermolecular contacts from 5D to the chromophore methyl and H5 are consistent for both drugs. In addition, very strong contacts from 4D to 6A are also observed in both cases. Although, the NOE cross-peaks from the A-ring to the DNA are consistently more prominent in the mithramycin complex than in the chromomycin complex, the drug contacts suggest that the A-ring is not displaced from the DNA strand in either drug complex. The smaller number of chromomycin A-ring to DNA contacts can be explained by the larger degree of cross-peak overlap in the chromomycin NOESY spectrum involving the A-hexose resonances. Thus, fewer DNA to chromomycin A-ring contacts could be identified.

The orientation of the C-ring to the D-ring and chromophore ring is also similar for the two drugs. Very strong NOE contacts between the 1D and 3C protons suggest that the relative position of the C- and D-rings is not altered significantly for mithramycin and chromomycin complexes. Similarly, 1C and 5C protons for both drugs have very strong contacts to the chromophore H2 proton. Furthermore, the large upfield shift in the 1D resonance of about 2 ppm is a strong indicator that the D-ring is positioned over its neighboring drug chromomycinone ring. This ring-induced upfield shift is fully consistent with all three drug complexes summarized in Figure 7.

The NMR evidence clearly shows that the mithramycin dimer distorts the typically B-conformation of d(ATGCAT)$_2$. In order for the minor groove of d(ATGCAT)$_2$ to accommodate the large drug dimer, significant changes in the shape of this groove must occur. The strongest NMR evidence for these changes is as follows: large deviations (>0.2 ppm) in the chemical shifts of several DNA protons (Table I); a much more prominent cross-strand contact between G3H1′ and A5H2 (Figure 2B); more prominent intrastrand contacts be-

tween G3H8 and C4H6 and between G3H2″ or G3H2′ and C4H6; very weak cross-peaks between the C4H6 and the C4H2′ and C4H2″ geminal protons; a change in the relative positions of the C4H2′ and C4H2″ chemical shifts. Overall these changes are coincident with those observed for the chromomycin complex and indicative of an unusual distortion near the cytosine nucleotide (Banville et al., 1990). The more prominent cross-strand contact between G3H1′ and A5H2 can be compared with the A-conformation of DNA where these protons are closer than in the B-DNA conformation (Arnott & Hukins, 1972; Wuthrich, 1986).

Conclusions

Mithramycin and chromomycin are remarkably similar in their binding properties to $d(ATGCAT)_2$. The 2:1 (drug/DNA duplex) stoichiometry, 2-fold symmetry, and slow chemical exchange properties of both complexes are further supported by very similar drug to DNA contacts. In both complexes, the DNA appears to be significantly distorted by drug binding, and both drugs are situated in or along the minor groove side of the duplex. However, several differences are apparent between these two complexes, such as the position of the B-hexose ring. In addition, a faster exchange rate for the mithramycin complex was observed, which suggests that mithramycin has a slightly lower affinity for the $d(ATGCAT)_2$ duplex than chromomycin.

References

Alden, C. J., & Kim, S.-H. (1979) *J. Mol. Biol. 132*, 411–434.

Arnott, S., & Hukins, D. W. L. (1972) *Biochem. Biophys. Res. Commun. 47*, 1504–1510.

Aue, W. P., Barthoholdi, E., & Ernst, R. R. (1976) *J. Chem. Phys. 64*, 2229–2246.

Baguley, B. C. (1982) *Mol. Cell. Biochem. 43*, 167–181.

Banville, D. L., Marzilli, L. G., & Wilson, W. D. (1986) *Biochemistry 25*, 7393–7401.

Banville, D. L., Keniry, M. A., Kam, M., & Shafer, R. H. (1990) *Biochemistry 29*, 6521–6534.

Behr, W., & Hartmann, G. (1969) *Biochem. Z. 343*, 519–527.

Behr, W., Honikel, K., & Hartmann, G. (1969) *Eur. J. Biochem. 9*, 82–92.

Berman, E., & Shafer, R. H. (1983) *Biopolymers 22*, 2163–2167.

Berman, E., Brown, S. C., James, T. L., & Shafer, R. H. (1985) *Biochemistry 24*, 6887–6893.

Bodenhausen, G., Vold, R. L., & Vold, R. R. (1980) *J. Magn. Reson. 37*, 93–106.

Brikenshtein, V. Kh., Pitina, L. R., Barenboim, G. M., & Gurskii, G. V. (1983) *Mol. Biol. 18*, 1606–1616.

Cons, B. M. G., & Fox, K. R. (1989) *Nucleic Acids Res. 17*, 5447–5459.

Corongiu, G., & Clementi, E. (1981) *Biopolymers 20*, 551–571.

Davis, D. G., & Bax, A. (1985) *J. Magn. Reson. 64*, 533–535.

Dwek, R. A. (1973) in *NMR in Biochemistry*, Clarendon Press, Oxford, U.K.

Fox, K. R., & Howarth, N. R. (1985) *Nucleic Acids Res, 13*, 8695–8714.

Gao, X., & Patel, D. J. (1989a) *Biochemistry 28*, 751–762.

Gao, X., & Patel, D. J. (1989b) *Q. Rev. Biophys. 22*, 93–138.

Hartmann, S. R., & Hahn, E. L. (1962) *Phys. Rev. 128*, 2042–2053.

Illarionova, R. P., Dykhovichnaya, D. E., & Bondarenko, B. N. (1970) *Antibiotiki (Moscow) 15*, 415–418 (Russian).

Jamin, N., James, T. L., & Zon, G. (1985) *Eur. J. Biochem. 152*, 157–166.

Kam, M., Shafer, R. H., & Berman, E. (1988) *Biochemistry 27*, 3581–3588.

Keniry, M. A., Brown, S. C., Berman, E., & Shafer, R. H. (1987) *Biochemistry 26*, 1058–1067.

Kennedy, B. J., Yarbo, J. W., Kickertz, V., & Sandberg-Wollbeim, M. (1968) *Cancer Res. 28*, 91–97.

Kersten, W., Kersten, H., & Szybalski, W. (1966) *Biochemistry 5*, 236–244.

Klevit, R. E., Wemmer, D. E., & Reid, B. R. (1986) *Biochemistry 25*, 3296–3303.

Marion, D., & Wuthrich, K. (1983) *Biochem. Biophys. Res. Commun. 113*, 967–974.

Miller, D. M., Polansky, D. A., Thomas, S. D., Ray, R., Campbell, V. W., Sanchez, J., & Keller, C. A. (1987) *Am. J. Med. Sci. 294*, 388–394.

Neuhaus, D., Wagner, G., Vasak, M., Kagi, J. H. R., & Wuthrich, K. (1985) *Eur. J. Biochem. 151*, 257–273.

Prasad, K. S., & Nayak, R. (1976) *FEBS Lett. 71*, 171–174.

Redfield, A. G., & Kunz, S. D. (1975) *J. Magn. Reson. 19*, 250–254.

Scott, E. V., Son, G., Marzilli, L. G., & Wilson, W. D. (1988) *Biochemistry 27*, 7940–51.

States, D. J., Haberkorn, R. A., & Ruben, D. J. (1982) *J. Magn. Reson. 48*, 286–292.

Thiem, J., & Meyer, B. (1979) *J. Chem. Soc., Perkin Trans. 2*, 1331–1336.

Thiem, J., & Meyer, B. (1981) *Tetrahedron 37*, 551–558.

Ulrich, E. L., John, E. M., Gough, G. R., Brunden, M. J., Gilham, P. T., Westler, W. M., & Markley, J. L. (1983) *Biochemistry 22*, 4362–4365.

Van Dyke, M. W., & Dervan, P. B. (1983) *Biochemistry 22*, 2372–2377.

Ward, D., Reich, E., & Goldberg, I. (1965) *Science (Washington, D.C.) 149*, 1259–1263.

Waring, M. (1970) *J. Mol. Biol. 54*, 247–279.

Wuthrich, R. (1986) in *NMR of Proteins and Nucleic Acids*, Wiley-Interscience, New York.

Zimmer, Ch., & Wahnert, U. (1986) *Prog. Biophys. Mol. Biol. 47*, 31–122.